Preliminary Experimental Investigation on the Geomechanical Behaviour of Hydrate-Bearing Fine-grained Sediments

Boning Ma, Jocelyn Hayley & Jeffrey Priest
Department of Civil Engineering – University of Calgary, Calgary, AB, Canada

ABSTRACT
The existence of gas hydrate within deep marine sediments influences the geomechanical properties of the host sediment. As such, dissociation of the hydrate, through ongoing climate change or through future production of the hydrate, may pose a significant risk to submarine slope stability. Although extensive research has been conducted on hydrate-bearing sands, very limited studies on geomechanical behaviour of gas hydrate-bearing fine-grained soils have been reported in the literature. This paper presents the initial results of a study to investigate the impact of hydrate veins on the K_0 compression of hydrate-bearing fine grained sediments. An experimental investigation was carried out using fine-grained soil specimens with cylindrical carbon dioxide hydrate-bearing sand cores to mimic natural hydrate vein-bearing fine-grained sediment. After formation of the hydrate, K_0 compression tests were carried out to explore differences in axial deformation of the specimens as a function of applied vertical stresses. Test results indicate that brittle yielding occurred during K_0 compressions due to the breakage of the bond between the hydrate and the host grains as well as the high content of stiff hydrate. The hydrate-bearing fine-grained specimen is capable of withstanding much greater axial loads than the baseline specimen. Before yielding, the axial load was primarily carried through the hydrate vein, while after yielding, the specimen behaviour approached that for the baseline case.

RÉSUMÉ
L'existence d'hydrates de gaz dans les sédiments marins profonds influence les propriétés géomécaniques des sédiments hôtes. En tant que tel, la dissociation de l'hydrate, à travers le changement climatique en cours ou à travers la production future de l'hydrate, peut poser un risque important pour la stabilité de la pente sous-marine. Bien que des recherches approfondies aient été menées sur les sables riches en hydrates, des études très limitées sur le comportement géomécanique des sols à grains fins riches en hydrates de gaz ont été rapportées dans la littérature. Cet article présente les premiers résultats d'une étude visant à étudier l'impact des veines d'hydrates sur la compression K0 de sédiments à grains fins contenant des hydrates. Une étude expérimentale a été réalisée en utilisant des échantillons de sol à grain fin avec des carottes cylindriques de sable contenant du dioxyde de carbone pour imiter des sédiments à veine fine riches en hydrates naturels. Après la formation de l'hydrate, des essais de compression K0 ont été effectués pour explorer les différences de déformation axiale des éprouvettes en fonction des contraintes verticales appliquées. Les résultats des tests indiquent que des casses fragiles se sont produites pendant les compressions K0 en raison de la rupture de la liaison entre l'hydrate et les grains hôtes ainsi que de la forte teneur en hydrate rigide. L'échantillon à grains fins contenant des hydrates est capable de supporter des charges axiales beaucoup plus grandes que l'échantillon de base. Avant de céder, la charge axiale était principalement transportée à travers la veine d'hydrate, tandis qu'après le rendement, le comportement de l'échantillon se rapprochait de celui du cas de base.

1 INTRODUCTION

Gas hydrates are solid, ice-like compounds composed of predominantly methane gas molecules that are encaged within water molecule lattice (Max et al., 2005; Nixon and Grozic, 2007; Waite et al., 2009). Relying on high pressure and low temperature to form and remain stable, the greatest volume of hydrate is distributed in marine continental slopes and margins, with a smaller proportion found in and below the permafrost in polar regions (Collett et al., 2009).

As a result of decades of research and exploration on these unique compounds, it has been suggested that despite its potential as a future energy solution, gas hydrate may pose a tremendous geohazardous threat, owing to the adverse effects of global warming and human exploitation on hydrate stability, in permafrost and marine regions (Maslin et al., 2010). An increase in ocean bottom temperature in the Arctic region is occurring faster and more severe compared to other global regions (Pierrehumbert, 2010). This rise in temperature can lead to hydrate dissociation, which can generate excess pore pressure in marine strata leading to gas chimneys, and mud volcanoes (Jia et al., 2016). The offshore oil and gas industry has observed well bore instability, unexplained gas bubbling, and gas blow-outs associated with gas hydrate after penetrating gas hydrate-bearing stratum when exploiting deeper conventional energy resources (Grozic, 2010). In addition, loss of stiff hydrate through dissociation can significantly weaken the host sediment (Bouriak et al., 2000; Paull et al., 2000; Nixon and Grozic, 2007; Priest et al., 2014). This may lead to massive landslides along continental margins (McIver, 1982; Kenvolden, 1993; Grozic, 2010; Priest et al., 2014) and can potentially trigger tsunamis.

Characterization of the geomechanical properties of gas hydrate-bearing sediments can help scientists understand and assess the risks that hydrate pose as a

geohazard. Using laboratory synthesized gas hydrate, researchers have conducted experimental tests to determine the geomechanical behaviour of gas hydrate-bearing sands (Waite et al., 2004; Ebinuma et al., 2005; Hyodo et al., 2005, 2008, 2009; Santamarina and Ruppel, 2010; Yoneda et al., 2016). Although, gas hydrate associated geotechnical research has mainly focused on hydrate-bearing coarse-grained sediments, over 90% of the hydrate in nature is formed within fine-grained sediments (Boswell and Collett, 2006). However, limited research has been carried out, or attempted, on gas hydrate-bearing fine-grained soils.

Yun et al. (2007) and Lee et al. (2010) prepared THF(Tetrahydrofuran)-water mixtures to form THF hydrates-bearing sediments and investigated the differences in volumetric behaviour between hydrate-bearing coarse-grained and fine-grained sediments. They showed that volumetric strain during gas hydrate formation and dissociation in low specific surface area sediments, such as sand, was much smaller than that in high specific surface area sediments, like clay.

Lei (2017) adopted a number of different strategies to synthesize hydrate within silts and clays. He conducted experiments with carbon dioxide and THF hydrate formation/dissociation as well as associated physical process. However, due to the limitation of the techniques, geomechanical testing of these hydrate-bearing specimens could not be performed.

The morphology of gas hydrate formed in fine-grained sediments varies due to factors such as grain mineralogy, temperature-pressure condition, salinity, and time (Collett et al., 2009), but typically occur in higher concentration in vertical and near vertical fractures as hydrate veins (Cook and Goldberg, 2008; Waite et al., 2009; Rees et al., 2011; Priest et al., 2014), as seen in Figure 1.

Focusing on hydrate vein-bearing sediments, Smith (2016) synthesized vertical, cylindrical, synthetic THF hydrate veins within fine-grained soil specimens to mimic hydrate structures observed in nature. Unconsolidated undrained tests and consolidated drained tests were carried out to determine the effect of differing vein sizes and effective confining pressure on the geomechanical behaviour of the hydrate vein-bearing soil. The limitation of his method was the difficulty in maintaining THF hydrate stability during tests as the hydrate easily dissolved into the sediment pore water, thus introducing error in the results. Wu (2016) improved on the methodology of Smith (2016) by using plastic wrap to isolate the veins from the sediment, thus preventing THF hydrate dissolution into the pore fluid. Although better insights into the effects of hydrate veins on geomechanical behaviour of fine-grained sediments were gained using this technique, the plastic wrap enveloping the hydrate may have affected the interaction between hydrate and soil particles.

It is evident from the above discussion that mechanical properties of hydrate vein-bearing fine-grained sediments needs further investigation in order to successfully predict the behaviour of such geomaterials as well as assess their role and mechanisms in triggering geohazards.

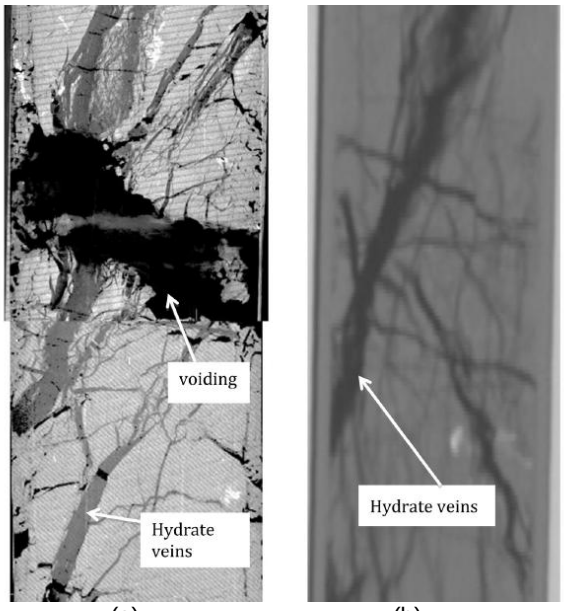

(a) (b)

Figure 1. Hydrate veins in fine-grained sediments: (a) X-Tek CT scanning of the core section after depressurization and subsequent freezing; (b) X-ray CT scan of the core section before depressurization (from Rees et al. (2011) and Priest et al. (2014)

As such, hydrate vein-bearing fine-grained specimens were artificially synthesized, and laboratory tests were carried out to investigate the geomechanical properties and behaviour of these specimens. The experimental programme as well as preliminary test results and discussion are presented in the following sections.

2 EXPERIMENTAL PROGRAMME

2.1 Scheme of the compound specimen

Natural hydrate veins are composed of complicated geometrical forms that increase the difficulty in synthesizing laboratory analogues. In our tests a compound specimen is configured, as seen in Figure 2. The specimen is formed of a fine-grained cylindrical soil sample with a coarse grained core. The coarse grained core provides sufficient permeability for hydrate formation, thereby serving as a mimic for the hydrate veins within fine-grained sediments.

The configured specimen is similar to that used in Smith (2016) and Wu (2016). However, in our study we form CO2 hydrate within the unsaturated sand core instead of using prefabricated THF veins. This allowed hydrate veins to be formed in-situ rather than being formed independently and then being inserted into the central void of the specimen prior to placing the sample in the test apparatus. In addition, CO2 dissociation leads to gas release and change in effective stress similar to that experienced in the field (THF has no gaseous phase during dissociation). This will enable further research to be conducted that can incorporate effective stress

changes on the geomaterial behaviour during hydrate dissociation.

2.2 Experimental Materials

A mixture of 80% Sil Industrial Minerals Flour 325 mesh ground silica and 20% EPK Kaolin, was prepared with liquid limit (LL) and plastic limit (PL) of 25% and 17%, respectively. Wisconsin sand from Red Deer, Alberta was used for the core material to form and host the gas hydrate. Carbon dioxide was chosen as the hydrate forming gas for this research because of its high solubility in water and lower pressure conditions required for hydrate formation.

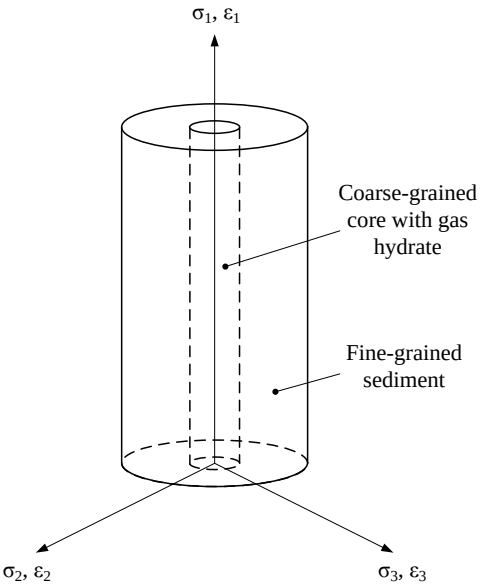

Figure 2. Schematic diagram of the compound specimen

2.3 Experimental Apparatus

The proposed research used a temperature controlled triaxial testing system, as seen in Figure 3, in which gas hydrate-bearing specimens can be synthesized and subsequent geomechanical tests carried out on the hydrate-bearing soil.

The apparatus is equipped with Advanced Pressure/Volume Controllers (ADVDPC) which allows pressure control up to 4MPa with 0.1kPa precision. Inside the cell an internal coil provides heating/cooling. A 50kN load frame with an internal load cell is used to measure the vertical load applied to the specimen. Global axial displacement of the specimen was measured by an external LDVT on the load ram. Local axial and radial displacements were measured though internal local LDVTs that are glued on the specimen, as seen in Figure 4.

2.4 Specimen Preparation

Soil specimens were prepared by first consolidating a soil slurry formed from silica flour and kaolin with distilled, de-aired water. The prepared slurry was then consolidated under a 1-D vertical load of 300 kPa in a cylinder measuring 20.5 cm internal diameter and 20 cm internal height. After full consolidation, soil specimens were taken by pushing 70 mm internal diameter sampling tubes into the prepared soil, with the specimens and tubes sealed in polyethylene bags and stored in a moisture room for future use. When specimens were required for testing, they were extruded from the tube and trimmed to a height of 140 mm.

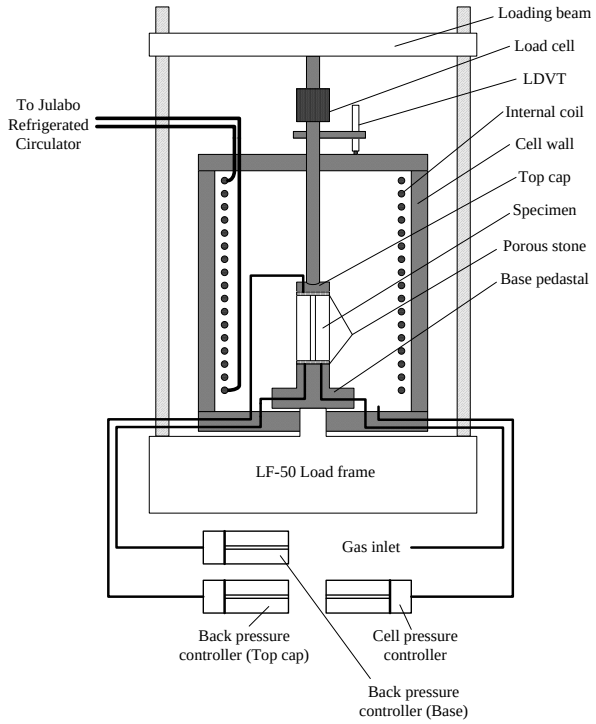

Figure 3. Schematic diagram of triaxial testing apparatus for hydrate-bearing soils

The void for the sand core was created using a drill press and a wood auger of 25.4 mm (1") diameter, forming a cylindrical hole in the center of the specimen. Then a frozen sand core 25.4 mm (1") diameter and 140mm height was inserted into the void. The sand core was prepared by tamping unsaturated sand into a split mould and subsequently freezing the sand. The water content of the sand core was 7.8% which equates to a degree of saturation of 35%.

2.5 Test procedure

In this study, K_0 compression tests were carried out on a clayey silt specimen without hydrate, providing a baseline test for comparison with a hydrate vein-bearing specimen. For the base line test the prepared specimen was isotopically consolidated to an effective stress of 50 kPa with a 2000 kPa back pressure. The system was then cooled down to 3°C. A Skempton's B-check (Skempton, 1954) was carried out, with a value of B = 0.96 calculated for the baseline specimen.

Several rounds of K_0 consolidation tests were performed. During the consolidation test, the back

pressure controller at the base of the sample was set to a constant 2000 kPa and allowed water to drain out of the sample, while the top cap measured the specimen pore pressure, such that the specimen was subject to one-way drainage during the consolidation processes. The K_0 consolidation was carried out through an isotropic increase in cell pressure (increase took 60 to 90 seconds to reach target value) while the back pressure was maintained at the set pressure. As the specimen consolidated due to the increase in effective stress the axial load was increased to maintain zero radial strain (as measured by the local radial LVDT). The effective confining stresses for each stage of the K_0 consolidation tests were 100 kPa, 200 kPa, 300 kPa, 400 kPa, 600 kPa, 800 kPa, 1000 kPa, 1600 kPa, and 1900 kPa, respectively. The vertical deformation, volume change, axial load, and pore pressure dissipation were measured and recorded.

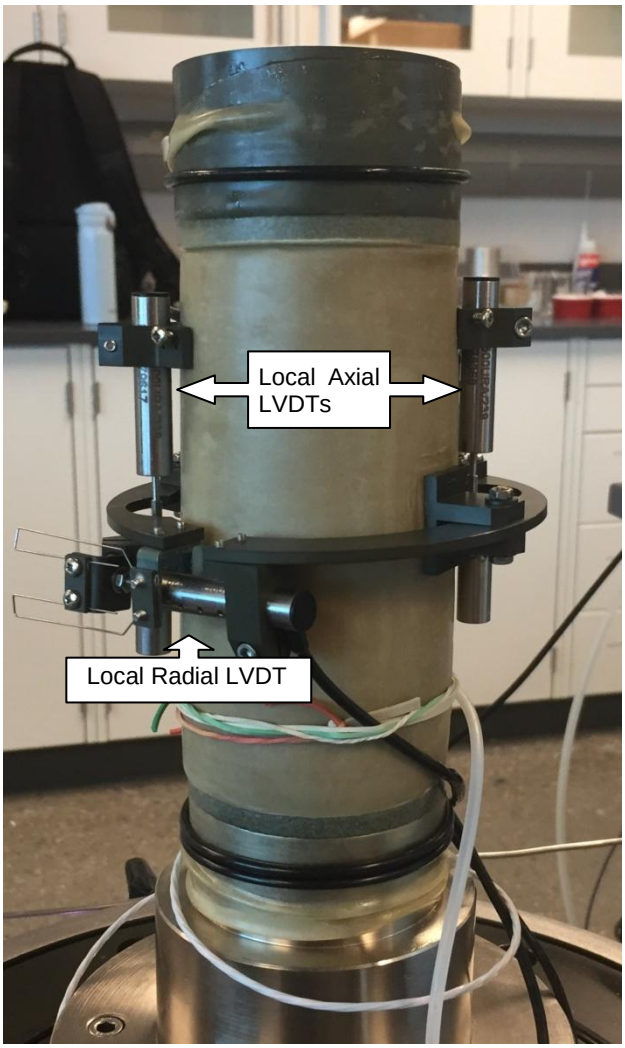

Figure 4. A photo of a specimen ready for test

The phase boundary for CO_2 hydrate and the pressure-temperature path for forming the hydrate-bearing specimen are shown in Figure 5. In this study, hydrate formation makes use of the 'excess gas' method (Priest et al., 2009) to synthesize carbon dioxide hydrate within the unsaturated sand core. Once the compound specimen was installed in the apparatus, the sand core was first flushed with CO_2 gas to replace the air within it. The cell pressure and pore gas pressure were increased up to 1850 kPa and 1820 kPa respectively ensuring a constant effective confining pressure. The temperature of the specimen was then reduced to 3°C. Once at this temperature, the cell pressure and pore gas pressure were simultaneously raised up to 3200 kPa and 3150 kPa, respectively. The system was left at this temperature and pressure for 55 hours for hydrate synthesis (CO2 gas was continually supplied as hydrate formed).

K_0 compression tests were conducted after this period of time to confirm the success of hydrate formation. Initial increases in effective confining stress were from 50 kPa to 250 kPa with 50 kPa increment. The specimen was then allowed to relax for 25 hours. During this stage, the temperature of the system was increased to 7°C, and K_0 recompression tests were subsequently performed with the effective confining stress increased to 350 kPa, 450 kPa, 550 kPa, and 650 kPa, respectively.

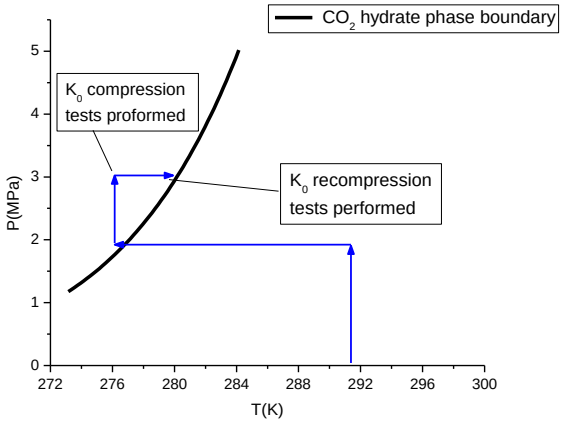

Figure 5. CO_2 hydrate phase boundary and the pressure-temperature path for the hydrate-bearing sample

3 TEST RESULTS AND DISCUSSION

As highlighted above, K_0 consolidation involved increasing cell pressure with the back pressure/volume controller holding a constant back pressure and allowing pore fluid to drain out of the specimen. Due to the low permeability of the clayey silt, drainage of the pore water for the baseline specimen took a period of time. Thus during the early period of each test a increase in excess pore water pressure (measured by the top pore pressure transducer) was observed due to the increase in total stress. Figure 6 shows the increase and subsequent dissipation of excess pore water pressure with time, during each K_0 consolidation stage for the baseline specimen. The initial increase in confining stress leads to a rise in pore pressure which reached a peak in 4 to 6 minutes, with subsequent dissipation of excess pore pressure due to pore water draining from the base of the

sample taking approximately 8 to 12 hours for the normally consolidated baseline specimen, although during the first stage (Eff. Cell P. increased from 50 kPa to 100 kPa) dissipation of pore pressure took ~3 hours as at this confining stress the soil was in over-consolidated state.

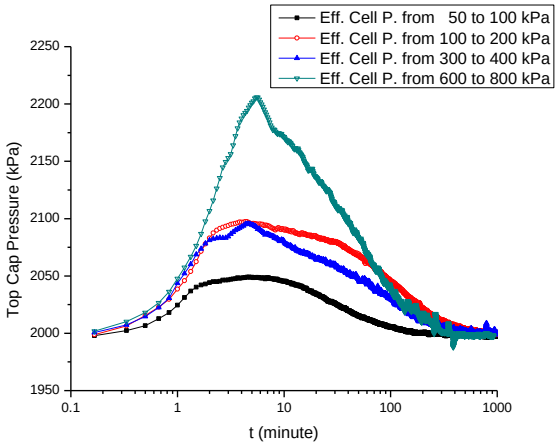

Figure 6. Increase and dissipation of excess pore water pressure of baseline specimen

The hydrate vein-bearing specimen was connected to the CO_2 gas source throughout the testing of this specimen, therefore, these specimens were not fully saturated and compressibility of the gas was such that no appreciable rise in pore pressure was observed. Future tests will be conducted using fully saturated specimens after hydrate formation, thereby enabling the any change in pore pressure to be monitored.

Changes in axial strain with effective axial stress for both specimens are shown in Figure 7. It can be seen that for the baseline specimen a reasonably small axial deformation occurred during the first loading with an gradual change in the slope of the consolidation line with the next stress increment. This specimen was formed by consolidating the soil slurry under a vertical 1-D stress of 300 kPa, which is greater than the initial stresses applied during K_0 consolidation, therefore the change in slope marks the transition from this over-consolidated state to the normally consolidated state (Casagrande, 1936) with an axial consolidation stress ~200 kPa (equating to a K_0 of 0.65). As the specimen is further consolidated past this stress the consolidation curve follows a straight line in the semi-log plot, therefore defining the normal consolidation line (NCL) for this soil.

In contrast, the hydrate vein-bearing specimen exhibited significantly different behaviour during K_0 compression. During the initial compression stages (red line, Figure 7) the radial LDVT did not detect any lateral deformation during the increase in total stress (up to 200kPa). As such, this specimen underwent isotropic compression. Once the effective confining stress was 250 kPa, radial deformation started to occur, and axial stress increased to maintain K_0 consolidation. Initially the axial deformation was minor for increases in effective axial stress up to 340 kPa. Once this stress was surpassed, yielding of the specimen started to occur with a significant change in slope of the consolidation line occurring (blue line, Figure 7). The yield stress σ_y' was determined to be 430 kPa using Casagrande method (Casagrande, 1936), significantly higher than the preconsolidation stress of the baseline specimen, showing that the hydrate vein-bearing specimen was stronger and stiffer than the baseline specimen. Beyond the yield stress the hydrate vein-bearing specimen exhibited considerable amounts of plastic deformation with the slope of the consolidation line being significantly steeper than that observed for the baseline test. Axial deformation took place quite abruptly, suggesting a brittle yielding behaviour. When the axial strain approached that observed for the baseline test (~5%) the axial displacement was stopped and the hydrate vein-bearing specimen was allow to relax from an effective axial stress of 1146kPa decreasing to 850 kPa. After this relaxation, K_0 compression was resumed for a further 4 stages of 100 kPa stress increments in effective confining stress. The subsequent 4 K_0 compression stages led to minor increases in both axial stress and deformation and followed that for the baseline test.

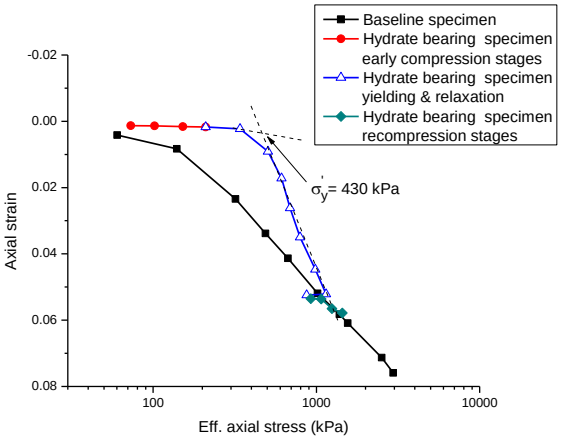

Figure 7. Axial strain versus effective axial stress of both specimens

The behaviour of the hydrate vein-bearing specimen is seen to be similar to that of structured or cemented soils. According to Ismail et al. (2002), the yielding pattern of cemented soils is a function of the strength and bonding mechanism of the cementing agent, with strongly cemented soils exhibiting brittle failure. The brittle yielding shown by the hydrate-bearing specimen is therefore likely the result of hydrate cementing of grain contacts within the sand core, enhanced by the large diameter vein and the high hydrate content used in this test.

Changes in the K_0 value of both specimens corresponding to increases in effective confining stress are shown in Figure 8. The K_0 value of the baseline specimen starts from an isotropic stress condition with K_0 = 1 and decreases to a nearly constant value of 0.6 with increasing effective axial stress, as seen in Figure 8. The gradually decreasing value for K_0 indicates a smooth

transition from isotropic compression to K_0 compression for the baseline specimen.

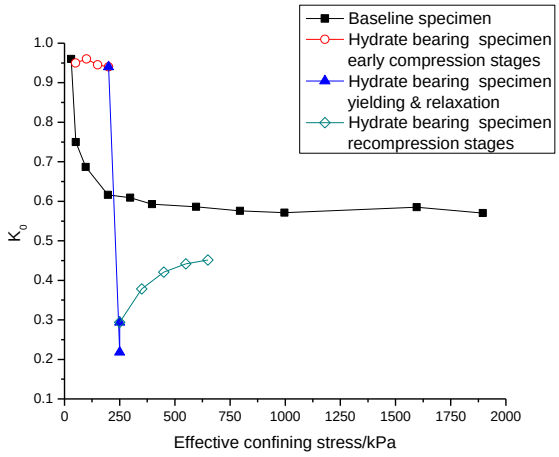

Figure 8. K_0 versus effective confining stress

However, for the hydrate vein-bearing specimen the K_0 value stays constant during the initial compression stages (highlighting the isotropic compression), and then decreases abruptly at a much higher stress level (250 kPa) highlighting the increased axial capacity of the hydrate vein-bearing specimen. After brittle failure and a period of relaxation the value of K_0 increases slightly during recompression although still much lower than the baseline case, indicating that after failure the hydrate vein is still contributing to the strength and stiffness of the specimen.

Figure 9 highlights the stress path, in q - p' space, followed by the two specimens tested. It can be seen that the stress path for the baseline test is linear and represents a typical K_0 line of the clayey silt specimen. The relationship between K_0 and the internal friction angle φ' presented by Jaky (1944) is given as

$$K_0 = 1 - \sin\varphi' \quad [1]$$

The K_0 consolidation test conducted on the baseline specimen resulted in an average value for $K_0 = 0.6$, which gives an internal friction angle φ' of 23.6°. In the framework of critical state soil mechanics (Roscoe, 1968),

$$\varphi' = \sin^{-1}\left(\frac{3M}{6+M}\right) \quad [2]$$

where M = q / p'. For the baseline test this corresponds to a critical state failure line (CSL) of slope M = 0.923, which is plotted in Figure 9. It can be seen that the baseline test lies significantly below the failure line of the soil.

In contrast, the stress path for the hydrate vein-bearing specimen varies significantly during the test. The initial isotropic loading can be seen by the horizontal stress path with q ~ 0 (red circles, Figure 9). It is expected that a drained specimen would experience radial shortening during loading. However it is believed that this specimen was acting in an 'undrained' manner at this stage due to the formation of a thin hydrate layer at the interface between surface of the clayey silt matrix and the top and bottom pedestal as well as the sand core, creating a reasonably impermeable barrier preventing drainage of the clayey silt soil matrix. Once the applied confining pressure was sufficiently large (at around 250kPa confining stress) it is assumed that the pore pressure difference between that within the soil matrix and the partially saturated sand vein was sufficient to break the hydrate barrier thus allowing drainage to occur, radial displacement to increase, leading to increase in axial stress to maintain k_0 conditions (blue triangles, Figure 9).

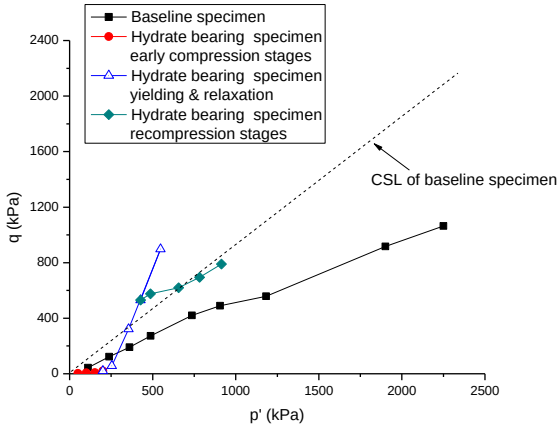

Figure 9. Stress paths of both specimens in q - p' plot

K_0 compression starts once the barrier is overcome, leading to significant increase in deviatoric stress with the gradient of the stress path greater than the CSL of the baseline specimen. The maximum deviatoric stress is significantly higher than that given by critical state framework highlighting the significant stiffness and strength enhancement that occurred due to CO_2 hydrate in the sand core. During the time the test was paused, the stress path reversed its direction as axial stresses decreased during the relaxation period. With subsequent recompression, the stress path remains higher than the baseline, although somewhat parallel to the baseline case, suggesting that the specimen was still stress hardening.

4 CONCLUSIONS

This paper highlights the results from preliminary tests carried out on hydrate vein-bearing fine-grained soil under K_0 consolidation. Significant differences in the geomechanical behaviour between a baseline test and the vein-bearing specimen were observed. The following conclusions can be drawn:

1) A successful method for forming gas hydrate within sand veins within fine-grained sediments was established.

2) During K_0 compressions of the hydrate vein-bearing specimen brittle yielding occurred, likely resulting from breakage of the bond between the hydrate and the host grains. This behaviour was enhanced due to the high

hydrate saturation within the sand and the large diameter of the sand vein.

3) Hydrate-bearing sand vein provides additional strength and stiffness to the sediment, compared to the baseline specimen without hydrate. Before yielding very little axial deformation is observed showing the axial load was primarily carried by the hydrate vein.

4) After yielding and period of relaxation the hydrate vein-bearing specimen approaches that for the baseline case under high effective stresses.

Further testing will be carried out using different vein diameters, including using saturated hydrate veins, to fully explore the impact of these hydrate veins on the K_0 consolidation of fine-grained soils. In addition, hydrate dissociation will be conducted at different stages of axial loading to understand the potential risks that dissociation of hydrates in nature (through global warming) may have on sediment stability.

REFERENCES

Boswell, R. and Collett, T. 2006. The gas hydrates resource pyramid. *Natural Gas & Oil*, 304: 285-4541.

Bouriak, S., Vanneste, M., and Saoutkine, A. 2000. Inferred gas hydrates and clay diapirs near the Storegga Slide on the southern edge of the Vøring Plateau, offshore Norway. *Marine Geology*, 163(1): 125-148.

Casagrande, A. 1936. The determination of pre-consolidation load and it's practical significance. *Proc. Int. Conf. Soil Mech. Found. Eng*. Cambridge, Mass., 1936(3): 60.

Collett, T. S., Johnson, A. H., Knapp, C. C., and Boswell, R. 2009. Natural gas hydrates: a review. *Natural gas hydrates—Energy resource potential and associated geologic hazards: AAPG Memoir* 89: 146-219.

Cook, A. E., and Goldberg, D. 2008. Extent of gas hydrate filled fracture planes: Implications for in situ methanogenesis and resource potential. *Geophysical Research Letters*, 35(15).

Ebinuma, T., Kamata, Y., Minagawa, H., Ohmura, R., Nagao, J., and Narita, H. 2005. Mechanical properties of sandy sediment containing methane hydrate. *Proceedings of Fifth International Conference on Gas Hydrates, ICGH 5,* 3037: 958-961.

Grozic, J. L. H. 2010. Interplay between gas hydrates and submarine slope failure. *Submarine mass movements and their consequences*. Springer, Netherlands.

Hyodo, M., Y. Nakata, N. Yoshimoto, and T. Ebinuma 2005, Basic research on the mechanical behavior of methane hydrate sediments mixture, *Soils and Found*ations, 45: 75–85.

Hyodo, M., Nakata, Y., Yoshimoto, N., and Yoneda, J. 2008. Shear strength of methane hydrate bearing sand and its deformation during dissociation of methane hydrate. *Proceedings of 4th International Symposium on Deformation Characteristics of Geomaterials*: 549-556.

Hyodo, M., Nakata, Y., Yoshimoto, N., Orense, R., and Yoneda, J. 2009. Bonding strength by methane hydrate formed among sand particles. *AIP Conference Proceedings*, 1145(1): 79-82.

Ismail, M. A., Joer, H. A., Sim, W. H., and Randolph, M. F. 2002. Effect of cement type on shear behavior of cemented calcareous soil. *Journal of Geotechnical and Geoenvironmental Engineering*, 128(6): 520-529.

Jaky, J. 1944. The coefficient of earth pressure at rest. *Journal of the society of Hungarian architects and engineers*. 355-358.

Jia, Y., Zhu, C., Liu, L., and Wang, D. 2016. Marine Geohazards: Review and Future Perspective. *Acta Geologica Sinica* (English Edition), 90(4): 1455-1470.

Kvenvolden, K. A. 1993. Gas hydrates–geological perspective and global change. *Reviews of Geophysics*, 31(2): 173-187.

Lee, J. Y., Santamarina, J. C., and Ruppel, C. 2010. Volume change associated with formation and dissociation of hydrate in sediment. *Geochemistry, Geophysics, Geosystems*, 11(3).

Lei, L. 2017. Gas Hydrate in Fine-grained Sediments—Laboratory Studies and Coupled Processes Analyses *Doctoral dissertation*, Georgia Institute of Technology, USA.

Max, M. D., Johnson, A. H., and Dillon, W. P. 2005. *Economic geology of natural gas hydrate*. Springer Science & Business Media.

Maslin, M., Owen, M., Betts, R., Day, S., Jones, T. D., and Ridgwell, A. 2010. Gas hydrates: past and future geohazard? *Philosophical Transactions of the Royal Society of London A: Mathematical, Physical and Engineering Sciences*, 368(1919): 2369-2393.

McIver, R. D. 1982. Role of naturally occurring gas hydrates in sediment transport. *AAPG bulletin*, 66(6): 789-792.

Nixon, M. F., and Grozic, J. L. 2007. Submarine slope failure due to gas hydrate dissociation: a preliminary quantification. *Canadian Geotechnical Journal*, 44(3): 314-325.

Paull, C. K., Ussler III, W., and Dillon, W. P. 2000. Potential role of gas hydrate decomposition in generating submarine slope failures. *Natural Gas Hydrate*. Springer, Netherlands: 149-456.

Pierrehumbert, R. T. 2010. *Principles of planetary climate*. Cambridge University Press.

Priest, J. A., Rees, E. V., and Clayton, C. R. 2009. Influence of gas hydrate morphology on the seismic velocities of sands. *Journal of Geophysical Research: Solid Earth*, 114(B11).

Priest, J. A., Clayton, C. R., and Rees, E. V. 2014. Potential impact of gas hydrate and its dissociation on the strength of host sediment in the Krishna–Godavari Basin. *Marine and petroleum geology*, 58: 187-198.

Rees, E. V., Priest, J. A., and Clayton, C. R. 2011. The structure of methane gas hydrate bearing sediments from the Krishna–Godavari Basin as seen from Micro-CT scanning. *Marine and Petroleum Geology*, 28(7): 1283-1293.

Roscoe, K. H. 1968. Soils and model tests. *Journal of strain analysis*, 3(1): 57-64.

Santamarina, J. C., and Ruppel, C. 2010. The impact of hydrate saturation on the mechanical, electrical, and thermal properties of hydrate-bearing sand, silts, and clay. *Geophysical Characterization of Gas Hydrates*,

Geophys. Dev. Ser, 14: 373-384.
Skempton, A. W. 1954. The pore pressure coefficients A and B. *Ceram. Trans*., 4(4): 143-147.
Smith, W. 2016. The Influence of Tetrahydrofuran Hydrate Veins on Fine-Grained Soil Behaviour. *MSc dissertation*. University of Calgary, Canada.
Sultan, N., Cochonat, P., Foucher, J. P., and Mienert, J. 2004. Effect of gas hydrates melting on seafloor slope instability. *Marine geology*, 213(1): 379-401.
Sultan, N., and Garziglia, S. 2011. Geomechanical constitutive modelling of gas-hydrate-bearing sediments. *The 7th International Conference on Gas Hydrates* (*ICGH 2011*).
Waite, W. F., Winters, W. J., and Mason, D. H. 2004. Methane hydrate formation in partially water-saturated Ottawa sand. *American Mineralogist*, 89(8-9): 1202-1207.
Waite, W. F., Santamarina, J. C., Cortes, D. D., Dugan, B., Espinoza, D. N., Germaine, J., ... and Soga, K. 2009. Physical properties of hydrate-bearing sediments. *Reviews of Geophysics*, 47(4).
Wu, J. 2016. The role of THF Hydrate veins on the geomechanical behaviour of hydrate-bearing fine grained soils. *MSc dissertation*. University of Calgary, Canada.
Yoneda, J., Jin, Y., Katagiri, J., and Tenma, N. 2016. Strengthening mechanism of cemented hydrate-bearing sand at microscales. *Geophysical Research Letters*, 43(14): 7442-7450.
Yun, T. S., Santamarina, J. C., and Ruppel, C. 2007. Mechanical properties of sand, silt, and clay containing tetrahydrofuran hydrate. *Journal of Geophysical Research: Solid Earth*, 112(B4).